Analysis and Comparison the elliptical and circular air hole PCF for chemical / bio-sensing application using 2D FDTD method

[1]N.Muduli [2]P.Sahu [3]S. Behera

[1,2,3]*Kalam Degree Science College Berhampur Odisha India*

Abstract:

We purpose to design two different liquid infiltrating PCF structure having elliptical and circular air holes in their cladding region. We examine three different liquid analyte like benzene, ethanol and water to infiltrate the fiber core and proper numerical investigation of pumped PCF is computed by the principle of 2D FDTD method including anisotropic perfectly matched layer as boundary treatment. The numerically calculated relative sensitivity are plotted versus wavelength by optimized various parameter of purposed PCF structure .The result reveals that higher sensitivity as a chemical sensor for low refractive index liquid analyte like benzene, ethanol and water. It also can be used to examine other essential properties like spot size, nonlinearity, beam divergence, confinement loss and V parameter so distinctly. The proposed elliptical air hole PCF enhances their higher sensitivity of 55.32%, 50.2% & 58.88% for ethanol, water and benzene respectively at an operating wavelength of 1.33µm. While circular air hole PCF enhances their higher sensitivity of 53.68%, 49.18% & 56.47% for same liquid analyte. In fact PCF structure having elliptical air holes in their cladding region shows more relative sensitivity over circular air hole PCF even though fabrication of elliptical PCF being very difficult. Hence selecting such PCF will play very important effective role in optical telecommunication and sensing purpose.

Keywords: *PCF, Chemical Sensor, Sensitivity, FDTD Method.*

I. Introduction

Optical sensor devices have been taken as an alternative to conventional solid-state planar, brittle, less flexible, and rigid electronic devices [1]. Electronic devices have some major limitations such as high manufacturing cost, complex procedure, slower response time and reliability as compared to the optical sensors. Electronic devices are also affected with electromagnetic (EM) and thermal noise or interference [2]. Now a days, physical sensing based on optical platform used to sense and monitor complex environment and its surrounding such as temperature, humidity, strain, stress, pressure, and torsion, etc. having important applications in wearable sensors, robotics, health and safety monitoring [3-8]. Therefore optical sensor devices have been found the suitable alternative for the gas, chemical and oil sensing applications, due to its advantages of low cost, less noise/interference, higher sensitivity, fast response, reliability, and compactness [9-11].

Since last decades, photonic crystal fiber has been shown great development in optical sensing [12-15]. Due to advance optical instrumentations, the field of fiber optics is no longer limited to telecommunication applications. PCF also known as holey fiber consists of periodically ordered microscopic cylindrical air holes running through the full length of the fiber. The standard PCF is made with fused-silica (SiO_2) that has a regular pattern of voids or air holes that run parallel to its axis. Unlike traditional optical fibers, both the core and cladding are made from the same material.

Of evolution in 1996 changed fields such as telecommunication and sensing, leading to the inception of high sensitivity and restrained systems based on light conveyance. This phenomenal innate of fiber optics such as geometric adaptability, increased sensitivity over extant techniques. And inherent amity with fibre optic communication technology makes them stand out for sensing application.

In this chapter, sensitivity and guiding properties of various index-guiding PCFs based gas/ chemical sensors as well as liquid sensors are extensively discussed. The finite difference time domain (FDTD) technique with perfectly matched boundary layer (PML) conditions are extensively used for the computational study of PCF based gas/ chemical sensors, as a result, we also described the PML effect on sensing. The important sensor parameters such as sensitivity and confinement loss effect due to change of pitch, number of rings, air-hole diameters, and air-filling fractions (AFF) are investigated. Recent advances of existing PCF based gas/chemical sensors are discussed, which consist of comparisons among several PCF structures in terms of relative sensitivity, and fabrication feasibility. Finally, research gaps of this field are addressed and potential future detections to overcome them are discussed.

In this work, we demonstrate the two PCF structure which offer higher relative sensitivity than in (16) for bio-sensing and chemical sensing. i.e both elliptical and circular air hole PCF structure have more sensitivity. In addition to this, we also analyze some different parameter like confinement loss, V parameter, spot size, beam divergence nonlinearity in briefly at an operating wavelength of 1.33µm. We include a perfectly matched layer in the outer in some micrometer which used to absorb the radiation energy to more accuracy. Numerical investigation can be carried out using Full Vectorial 2D FDTD method. This article is summarised as follows PCF structure in Sec-2, Mathematical analysis investigated in Sec-3, simulation result and discussion in briefly explained in Sec-4 and followed by conclusion and reference in Sec-5 and Sec-6 respectively.

II. Purposed PCF Structure

To enhance the feasibility of real operation the simple purposed PCF structures are designed as shown in Fig-1. The fiber having 3 air hole ring in their cladding formed as hexagonal shape and acts as dielectric medium. We have purposed to design two PCF structure having elliptical and circular air holes in their cladding and analyze the effect of chemical and bio-sensing purpose. The first, 2nd and 3rd air hole ring were fabricated with 6, 12, 18 elliptical and circular air holes. The diameter of cladding region is same for circular air hole ring and different for elliptical air hole rings.

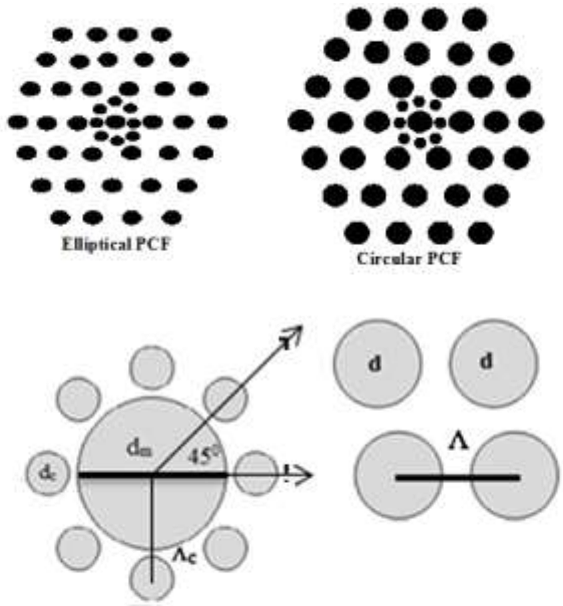

Fig-1

The distance between centre to centre of air hole is called lattice pitch denoted by Λ. Choosing pure silica as a background material of said proposed PCFs for novel optical behaviour. The lattice pitch of outer most region of cladding is set to Λ=3/4 d µm. The centre of core is filled up by one elliptical and circular air hole where diameter is set to d_c= 14/15 d µm. The centre of core of PCF surrounded by 8 air hole rings is to be chosen. The lattice pitch of core region is set to Λ_c=49/75 d µm. The diameter of each air hole is denoted by d_m. Air hole on the single core ring is rotated at an angle 45^0 and central core region is immersed with ethanol(µ=1.354), benzene(µ=1.366) and water(µ=1.33). The mode field pattern of proposed PCFs along X and Y axis polarised mode are shown in Fig-2(i, ii) at an operating wavelength of 1.33µm.

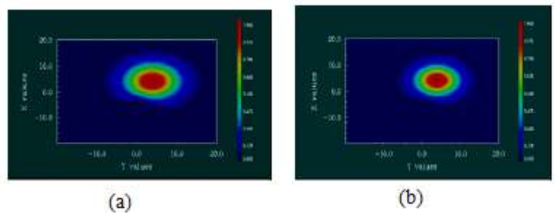

Fig.2 i) Mode field distribution pattern of designed circular PCF (a) X-polarization (b) Y-polarization.

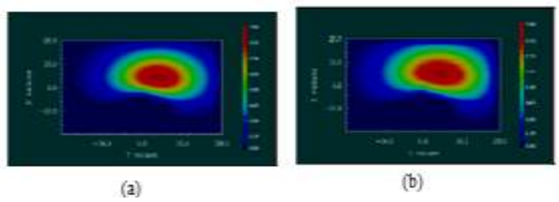

Fig.2.ii) Mode field distribution pattern of designed elliptical PCF (a) X-polarization (b) Y-polarization.

III. Mathematical Analysis

In order to study the field profile pattern of proposed hexagonal PCF structures of elliptical and circular air hole in cladding region to be investigated and by implementing 2D-FDTD technique. Considering the material is isotropic, linear, and lossless, the time dependent Maxwell's equations can be written as

$$\frac{\partial H}{\partial t} = \frac{1}{\mu(r)} \nabla \times E \qquad (1)$$

$$\frac{\partial E}{\partial t} = \frac{1}{\varepsilon(r)} \nabla \times H - \frac{\sigma(r)}{\varepsilon(r)} E \qquad (2)$$

E, H are electric field and magnetic field.
Where $\varepsilon(r)$, $\mu(r)$, $\sigma(r)$ are permittivity, permeability and conductivity of the material and all are in the function of position.
Equations (1) and (2) can be discretized using Yee's technique. Considering spatial and time discretization, equations (1) and (2) can be written for TE polarization as follows:

$$H_{x(i,j)}^{n+1/2} = H_{x(i,j)}^{n-1/2} - \frac{c\Delta t}{\mu\Delta y}\left(E_{z\left(i,j+\frac{1}{2}\right)}^{n} - E_{z\left(i,-\frac{1}{2}\right)}^{n}\right)$$
(3)

$$H_{y(i,j)}^{n+1/2} = H_{y(i,j)}^{n-1/2} + \frac{c\Delta t}{\mu\Delta x}\left(E_{z\left(i+\frac{1}{2},j\right)}^{n} - E_{z\left(i-\frac{1}{2},j\right)}^{n}\right)$$
(4)

$$E_{z(i,j)}^{n+1} = E_{z(i,j)}^{n} + \frac{c\Delta t}{\varepsilon\Delta x}\left(H_{y\left(i+\frac{1}{2},j\right)}^{n+\frac{1}{2}} - H_{y\left(i-\frac{1}{2},\right)}^{n+\frac{1}{2}}\right) - \frac{c\Delta t}{\varepsilon\Delta y}\left(H_{x\left(i,j+\frac{1}{2}\right)}^{n+\frac{1}{2}} - H_{x\left(i,j-\frac{1}{2}\right)}^{n+\frac{1}{2}}\right) \quad (5)$$

For stability, the time step $\Delta t \leq \frac{1}{c\sqrt{\Delta x^{-2}+\Delta y^{-2}}}$, where Δt the time increment, c is the velocity of light, Δx be the lattice increment in x direction, Δy be the lattice increment along y direction.

Considering equation (3),(4) and (5) , we have calculated the field distribution of PCFs in TE polarization mode.

For a nonlinear optical waveguide having Kerr-type non-linearity related permittivity ε_r depends on electric field E_y and can be expressed as

$$\varepsilon_r = \varepsilon_{r.L} + \alpha\left|E_y\right|^2 \quad (6)$$

Where $\varepsilon_{r.L}$ is the linear relative permittivity and α is the non linear co-efficient. A hybrid implicit FDTD method is used to simulate the field for 2D PCS with nonlinear rods. The overall stability of this hybrid FDTD scheme is determined by the stability in the linear medium regions. Consequently, nonlinearity in the structure does not effect stability and hence the grid size and time step.

The cladding region consists of finite number of air holes so it may cause the leakage of light. This leakage of light from core to exterior material results the confinement loss (dB/km), that can be expressed as:

$$\text{Confinement loss} = 8.686 k_0 I_m [n_{eff}] \text{ dB/km} \quad (9)$$

Where I_m is the imaginary part, n_{eff} is the effective index of x polarized and y polarized fundamental mode.

The relative sensitivity coefficient measures the interaction between the light and the analyte to be sensed. This interaction is measured through the absorption coefficient at a particular wavelength. According to the Beer-Lambert law, light is attenuated by the intensity of absorption of evanescent wave [17].

$$I(\lambda) = I_0(\lambda)\exp[-r\alpha_m l_c]$$

The absorbance of the sample to be detected is defined by the following equation:

$$A = \log\left(\frac{I}{I_0}\right) = r\,\alpha_m\,l_c$$

where I and I_0 are the input and output intensities, respectively, and c is the concentration of absorbing material. The length of the channel is l. The function of absorption coefficient is $\alpha_m(\lambda)$, and r is the relative sensitivity coefficient, which can be defined by the following equation [18].

$$r = \frac{n_r}{n_{eff}} f$$

where n_r refers to the refractive index of the sample to be sensed, and n_{eff} is the effective index of the guided mode, f is the fraction of total power located in the core, and it is also known as a power distribution function [19] by using Poynting's theorem which can be expressed as the following equation:

$$f = \frac{\int Re\left(E_x H_y - E_y H_x\right)dxdy}{\int Re\left(E_x H_y - E_y H_x\right)dxdy} \times 100$$

, where numerator integration for sample and denominator integration for total.

where E_x and H_x are transverse electric field and respectively; E_y and H_x are longitudinal electric field and magnetic field respectively. The f measures the % of energy which present in the holes.

IV. Result Analysis and Discussion

In order to improve the relative sensitivity and other parameter like confinement loss, spot size, V parameter, nonlinearity and beam divergence etc, we have purposed to design two PCF structure of different air hole size having background material silica in which inner core region is doped with benzene as shown in Fig.3.

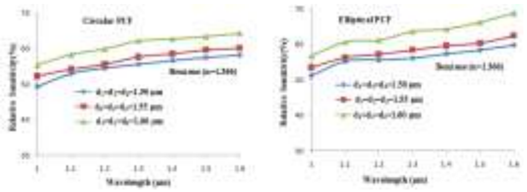

Fig.3 relative sensitivity versus wavelength for benzene proposed PCF

This Fig.3 maps out the relative sensitivity versus wavelength for different outer diameter of air hole. The results reveal that, with increasing the diameter of outer air hole, the relative sensitivity enhance their value, e.g the simulation result suggests that sensitive response increase from 57.52 to 62.38% at an operating wavelength of 1.33µm with in infrared region of outer air hole diameter $d_1=d_2=d_3=1.5$µm, $d_1=d_2=d_3=$ 1.55µm and $d_1=d_2=d_3=1.60$µm respectively for circular air hole PCF,. However the relative sensitivity response increases from 60.12 to 64.82% at a same operating wavelength and under same condition for elliptical air hole PCF. It is found that elliptical air hole PCF has more relative sensitivity response over circular air hole PCF at same condition using 2D FDTD method. It is also observed that the diameter $d_1=d_2=d_3=1.6\mu m$ of purposed PCF offers the greater sensitivity for both circular and elliptical PCF. But however the relative sensitivity of circular PCF is 62.38% while that of elliptical PCF is 64.82%.

Furthermore to discuss the polarisation characterstics of PCF strictly, we have investigated a PCF core filled with ethanol to measure the same sensitivity property. The inset Fig.4 represents the variation of relative sensitivity versus wavelength range and it offers, the response of relative sensitivity to maintain 54.5% at an operating wavelength of 1330nm for circular PCF structure while 56.2% for elliptical PCF structure when outer air hole diameter is set to $d_1=d_2=d_3=1.5\mu m$. By increasing the same outer air hole diameter from $d_1=d_2=d_3=1.55\mu m$ and $d_1=d_2=d_3=1.6\mu m$ respectively, the relative sensitivity increase from 60.2 to 62.42% for circular air hole PCF and 62.4 to 63.83% for elliptical air hole PCF.

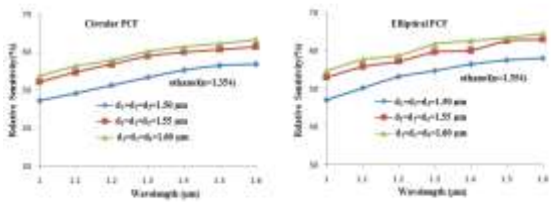

Fig.4 relative sensitivity versus wavelength for ethanol PCF

In fact relative sensitivity response basically depends on larger air hole diameter in the cladding region. As long as air hole diameter increases in cladding region, sensitivity response enhanced. Furthermore we have investigated another PCF structure with infiltrated the liquid analyte having refractive index 1.33. The Fig.5 depicts that the variation of relative sensitivity versus same wavelength range. It reports sensitivity gradually exponential increases with increase of wavelength and it gains 49.25% sensitivity choosing diameter of air hole set to $d_1=d_2=d_3=1.5\mu m$ for circular air hole PCF and it enhances the response of sensitivity to 54.62% as increasing the air hole diameter from $d_1=d_2=d_3=1.5\mu m$ to $d_1=d_2=d_3=1.6\mu m$, while relative sensitivity response somehow different for elliptical air hole PCF. It also gradually increases the sensitivity with increasing wavelength. It suggests that, the sensitivity 51.43% for $d_1=d_2=d_3=1.5\mu m$ and increase from 57.62 to 63.75% for $d_1=d_2=d_3=1.55\mu m$ and $d_1=d_2=d_3=1.6\mu m$. It may be noted that, the sensitivity has been improved significantly by implementing various air hole diameter in cladding region of PCF structure.

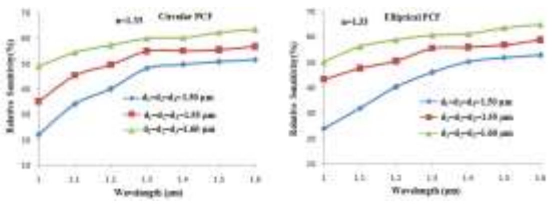

Fig.5 relative sensitivity versus wavelength for water proposed PCF

From above result, it concludes that the higher refractive index of liquid analyte offers higher sensitivity over lower refractive index keeping other parameter constant. Apart from this, elliptical air hole PCF shows higher sensitivity response over circular air hole PCF under same operating wavelength.

Fig.6 maps out the comparison of sensitivity response for three different liquid analyte such as $\mu=1.33$(water), $\mu=1.354$(ethanol) and $\mu=1.366$(benzene). We make sure that from simulation result, there are nearly identical curve for both PCF and estimated that higher refractive index liquid analyte shows high sensitive response at same operating wavelength. (e.g circular PCF shows 56.48% sensitive response while 58.85% for elliptical PCF) But it is interesting that elliptical air hole PCF shows more response of sensitivity than circular air hole PCF.

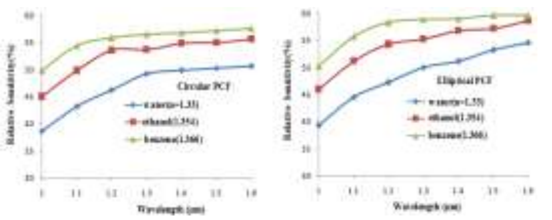

Fig.6 relative sensitivity versus wavelength for three different liquid analyte.

In addition, during the fabrication of PCF structure, a small amount of fault may occur unknowingly and fabrication of PCF structure is a vital role due to which it measures the capability of fault tolerance. We measure the relative sensitivity curve for two different liquid anlalyte (water and ethanol) due to variation of air hole diameter from ±1% to ±2% with the optimum sensitivity curve. It is also observed that air hole with diameter -1% and -2% offers higher sensitivity over the optimum sensivity curve and at the same time +1% and +2% provides lower sensitivity over optimum sensivity curve. Similarly the relative sensitivity curve for liquid analyte water($\mu=1.33$) of air hole diameter variation from ±1% to ±2% along with optimum sensitive curve, here air hole diameter with -1%, -2% and +2% suggest higher sensitivity over the optimum sensitivity curve and -1% provide lesser sensitivity than optimum sensitivity curve. It is found that, sensitivity increases with wavelength and air hole diameter (-2%) of proposed two PCF structure show the higher sensitivity for water, ethanol and benzene in both PCF structure. It is noticed that, elliptical PCF has more sensitive than circular one for all choosing parameters. The graphical representation of above result is not shown in fig. But it is found that , our proposed PCF structure show better result than (20,21) in chemical and bio-sensing purpose.

A PCF has used for various types of sensing approach like temperature, pressure, electrical, mechanical thermal energy chemical and bio-sensing etc. Among which chemical and bio-sensing are one of them, where we have analysed. It can be used as a sensor for remote sensing and nearest sensing approach. For remote sensing, a PCF should be single mode operation, at the same time multimode PCF is also able for nearest sensing application. A PCF can be single mode or multimode depending on most important characteristics by one more parameter called V number i.e. normalized frequency of fiber. The V number is denoted by the relation as follows:

$V=\frac{2\pi a}{\lambda}\sqrt{n_1^2-n_2^2}$, Where a= radius of the core. As V no enhances their value more and more, so it exposes the multimodal characteristics. Fig.7 plots the variation of V parameter versus wavelength for different liquid analyte. It decreases nearly exponential with increasing wavelength and slope making downward. The V no curve for water, ethanol and benzene reports that water is less V no than ethanol and benzene both elliptical and circular air hole PCF. But V no is more effective for elliptical air hole PCF over circular one. The spot size evaluation of PCF structure is most useful for fiber design and optical communication.

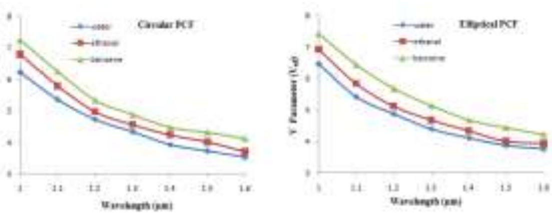

Fig.7 V parameter (V_{eff}) versus wavelength for circular and elliptical PCF

In order to obtain the spot size determination of PCF because it is important significant parameter for nonlinearity, bending loss, splice loss, beam divergence, coupling coefficient for fiber design and optical communication. Fig.8 represents spot size versus wavelength range and spot size curve is upward i.e. nearly exponential increasing with increase of wavelength among three liquid analyte for both elliptical and circular air hole PCF structure.

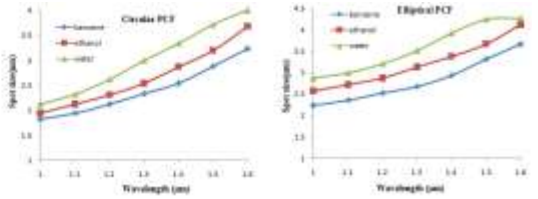

Fig.8 Spot size versus wavelength for both circular and elliptical PCF

It reports that, PCF having lower wavelength offers comparatively lower spot size than larger one on both elliptical/ circular air hole PCF structure. It is also found that PCF having lower wavelength(1 µm) shows comparatively lower spot size than wavelength of 1.7 µm and more.

Furthermore, we continue to investigate the beam divergence is a important key parameter of how fast beam spreading from the beam waist and it is directly link with the beam quality. The high value of beam divergence causes the less beam quality/beam focussing. Beam intensity is also lower with increasing beam divergence. Fig.9 shows the beam divergence versus wavelength range and it is seen that beam divergence linearly raised with increasing the wavelength within IR range. It is also found that elliptical air hole PCF has more linear raised over circular PCF one and the beam divergence θ =19^0 is found in a wavelength of 1.33µm. The high nonlinear coefficient of index guiding PCF makes it attractive for many nonlinear application of which SC generation has been interestingly investigated.

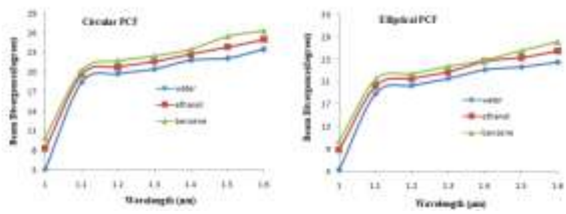

Fig.9 Beam Divergence versus wavelength for both circular and elliptical PCF.

Now a day PCF with high nonlinear coefficient is fully demanded. Fig.10 shows the nonlinear coefficient versus wavelength range. In ref.(22), a proposed PCF structure which had nonlinear coefficient =39.33$W^{-1}km^{-1}$ at an operating wavelength of 1.31μm. But our proposed two different PCF structure shows the nonlinear coefficient of 59.72 $W^{-1}km^{-1}$ for elliptical air hole and 57.63 $W^{-1}km^{-1}$ for circular air hole at same wavelength. Our proposed fiber is 1.5 times goood result than (23). This result seems to be proved that it has high nonlinear coefficient γ than the previous one (23). Based on above result, it truely signifies that our proposed two different PCF structure showed a modern technology in the area of optical communication and photonic device.

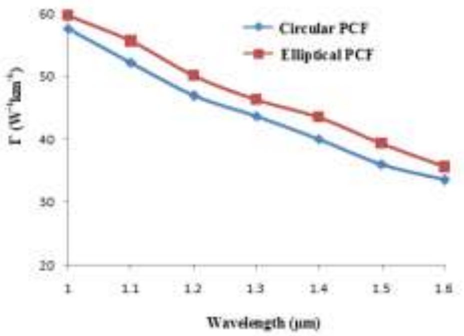

Fig.10 Nonlinear Coefficient Versus wavelength for circular and elliptical PCF.

Conclusion

In summary, a simple proposed two single polarisation PCF structure having elliptical and circular air hole in their cladding are investigated. However proposed PCFs analyzed and compare the improvement of chemical and bio sensing arena. The result shows that elliptical air hole PCF structure have more sensing character over circular air hole PCF structure using 2D FDTD method. The relative sensitivity about 64.82% for elliptical air hole PCF and 62.38% for circular air hole PCF at an operating wavelength of 1.31μm.

Reference

[1] D. Ahuja and D. Parande, "Optical sensors and their applications," Journal of Scientific Research and Reviews, vol. 1, pp. 060-068, 2012.

[2] Dorothee Grieshaber etal."Electrochemical Biosensors - Sensor Principles and Architectures" Sensors (Basel). 2008 Mar; 8(3): 1400–1458

[3] Ralf D. Pechstedt "Fiber optical sensors for aircraft applications" Proceedings of SPIE - The International Society for Optical Engineering 9226 · September 2014.

[4] Bichitra Nanda Sahoo "Hybrid functional microfibers for textile electronics and biosensors" J. Semicond. Volume 39 Issue 1

[5] Byeong Wan An" Smart Sensor Systems for Wearable Electronic Devices" Polymers 2017, 9, 303.

[6] Cheng Chi" Recent Progress in Technologies for Tactile Sensors" Sensors 2018, 18, 948.

[7] Chi, Z.; Shida, K. A new multifunctional three-dimensional tactile sensor using three coils. Jpn. J. Appl. Phys.2004, 43, 1638–1643

[8] Lee, J.S. eta " Highly Sensitive and Multifunctional Tactile Sensor Using Free-standing ZnO/PVDF Thin Film with Graphene Electrodes for Pressure and Temperature Monitoring" Sci. Rep. 2015, 5, 1–8.

[9] W. Ding, Y. Jiang, R. Gao, and Y. Liu, "High-temperature fiber-optic Fabry-Perot interferometric sensors," Review of Scientific Instruments, vol. 86, p. 055001, 2015.

[10] S. Asaduzzaman, B. K. Paul, and K. Ahmed, "Enhancement of sensitivity and birefringence of a gas sensor on micro-core based photonic crystal fiber," in Electrical Engineering and Information Communication Technology (ICEEICT), 2016 3rd International Conference on, 2016, pp. 1-4.

[11] Y. Liu and H. Salemink, "All-optical on-chip sensor for high refractive index sensing in photonic crystals," EPL (Europhysics Letters), vol. 107, p. 34008, 2014

[12] Q. Liu, S. Li, H. Chen, Z. Fan, and J. Li, "Photonic crystal fiber temperature sensor based on coupling between liquid-core mode and defect mode," IEEE Photonics Journal, vol. 7, pp. 1-9, 2015.

[13] Qiang Liu "Photonic Crystal Fiber TemperatureSensor Based on Coupling BetweenLiquid-Core Mode and Defect Mode" IEEE Photonics Journal Volume 7, Number 2, April 2015.

[14] Y. Lu, M. Wang, C. Hao, Z. Zhao, and J. Yao, "Temperature sensing using photonic crystal fiber filled with silver nanowires and liquid," IEEE Photonics Journal, vol. 6, pp. 1-7, 2014.

[15] K. Ahmed and M. Morshed, "Design and numerical analysis of microstructured-core octagonal photonic crystal fiber for sensing applications," Sensing and Bio-Sensing Research, vol. 7, pp. 1-6, 2016.

[16] H. Ademgil, S. Haxha, Highly birefringent nonlinear PCF for optical sensing of analytes in aqueous solutions, Optik – Int. J.Light Electron Opt. 127 (16) (2016) 6653–6660.

[17] M.F.H. Arif, K. Ahmed, S. Asaduzzaman, M.A.K. Azad, Design and optimization of photonic crystal fiber for liquid sensing applications, Photonic Sens. 6 (3) (2016) 279–288.

[18] A. Agrawal, N. Kejalakshmy, B.M.A. Rahman, K.T.V Grattan, Soft glass equiangular spiral photonic crystal fibe for supercontinuum generation, IEEE Photon. Technol. Lett. 21 (22) (2009) 1722–1724.

[19] W. Cai et al, Dodecagonal photonic quasi-crystal fiber with high birefringence, J. Opt. Soc. Am. A 33 (10) (2016) 2108.

[20] S. Asaduzzaman, K. Ahmed, T. Bhuiyan, T. Farah, Hybrid photonic crystal fiber in chemical sensing, Springer Plus 5 (1) (2016).

[21] S. Asaduzzaman, M.F.H. Arif, K. Ahmed, P. Dhar, Highly sensitive simple structure circular photonic crystal fiber based chemical sensor, in: 2015 IEEE International WIE Conference on Electrical and Computer Engineering (WIECON-ECE),

[22] D. Paul, R. Biswas, N.S. Bhattacharyya, Modal parameter analysis for crown glass and phosphate glass photonic crystal fiber, Indian J. Phys. 89 (7) (2015) 737–741.

[23] M.F.H. Arif, M.J.H. Biddut, A new structure of photonic crystal fiber with high sensitivity, high nonlinearity, high birefringence and low confinement loss for liquid analyte sensing applications, Sens. Bio-Sens. Res. 12 (2017) 8–14.